Raikunen, Joni; Avi, Eero; Remes, Heikki; Romanoff, Jani; Lillemäe-Avi, Ingrit; Niemelä, Ari

# Optimisation of passenger ship structures in concept design stage

*Published in:*
Ships and Offshore Structures

*DOI:*
10.1080/17445302.2019.1590947

Published: 03/10/2019

*Document Version*
Peer-reviewed accepted author manuscript, also known as Final accepted manuscript or Post-print

# Optimization of Passenger Ship Structures in Concept Design Stage

Joni Raikunen[a], Eero Avi[a], Heikki Remes[b], Jani Romanoff[b], Ingrit Lillemäe-Avi[a], Ari Niemelä[a]

[a]*Meyer Turku Oy, Telakkakatu 1, Turku 20240, Finland*

[b]*School of Engineering, Aalto University, Otakaari 4, Espoo 02150, Finland*

Corresponding author: Joni Raikunen. Tel.: +358 400 653 440. E-mail address: joni.raikunen@meyerturku.fi

**Abstract:** This paper presents an optimization method for concept design state of passenger ship with focus on utilisation of efficient Finite Element Modelling, evolutionary optimisation algorithm and indirect constraint relaxation. The response is analysed using 3D coarse mesh global finite element (FE) model, where stiffened panels are modelled using equivalent single layer (ESL) elements that follow the first order shear deformation theory. For traditional stiffened panel, the element has three layers, first represents the plate, second the stiffener web and third the stiffener flange. The web frames and girders are modelled with offset beam elements that can model any beam cross-section according to first order beam theory. The simplifications on stiffened panels and beams enable exploration of design space without changing the FE-mesh. As the focus is on conceptual design, the strength is defined based on the analytical formulations from classification society rules. In order to reach lightweight design, local stress peaks are allowed to exceed the rule-based strength limits, i.e. stress constraints are relaxed indirectly. Instead of increasing the allowed stress levels, the amount of material exceeding strength criteria is utilised. This approach results from production requirements where the area of local strengthening is of interest. The influence of this area on the optimization result is investigated and discussed. Optimization is based on Particle Swarm Optimization (PSO) algorithm. The method is applied for a prismatic cruise ship model and objective is to reduce the steel weight. The results show that stress relaxation has significant effect on the obtained total mass.

**Keywords:** optimization; equivalent single layer (ESL) theory; equivalent element; particle swarm optimization; global finite element model; passenger ship; constraint relaxation

## 1. Introduction

The size and structural complexity of passenger, and especially, cruise ships has increased during the last decades. This has led to increased scantlings and eventually mass, but also for more complex shape and architectural solutions. On the other hand, harsh competition in becoming more energy efficient and environmentally friendly is driving the ship owners' demand for lighter ships. As a result, more accurate and efficient calculation methods are needed to predict the structural performance already in early design phases, where most of the important decisions are made in limited time frame. Passenger ship conceptual design is typically performed using practical design methods such as classification society rules and Finite Element Analyses. The rules are simple and fast to use, but as they are implemented to many ship types, they usually contain methods which are not suitable for passenger ships with complex geometry and load-carrying mechanism. Therefore, the

resulting design may not be the most efficient, safe and a lot of extra steel will be used in the structure. Therefore, Hughes et al. (1980) recommended rational based design methods for ship structures to increase the structural performance. This approach is been considered the only feasible method in case of passenger ships (ISSC, 1997). The method consists of three phases: response analysis, strength evaluation and structural optimization. This paper focuses on response analysis with efficient Finite Element Analysis and Structural Optimization by use of evolutionary, global search algorithm and constrain relaxation defined by production constraints. This combination enables efficient exploration of structural design space affected by architectural, production and end-user requirements. Management of these requirements and their variation over design process is of fundamental importance in ever more competitive business of passenger ship design and construction.

The classical approach to calculate ship response during optimization is to use two-dimensional extrusions of the main frame and analyse it with classical beam theory. Local strength of the plate field can be defined according classification society rules like has been done by Rigo (2009), Sekulski (2009), Hirakawa et al. (2011) and Na and Karr (2013). The classical beam theory is valid for box-like ships like tankers, bulkers and barges, where the bending stresses are linearly distributed across the height of the cross section. Vasta (1958), Fransman (1988) and Heder and Ulfvarsson (1991) showed that the hull girder of a passenger ship with long deckhouse does not behave according to Euler-Bernoulli beam theory. This is mainly because of the shear lag effect, which is caused by hull-superstructure interaction and large side openings. Typically, the 2-dimensional optimization models are extended to cruise ships by using pre-defined superstructure efficiency parameters, e.g. Richir et al. (2007), Zanic et al. (2007) and Caprace et al. (2010). These are based on a separate Finite Element (FE) analysis and an assumption that the obtained normal strain distribution does not change considerably between design alternatives. However, this is not valid in optimization cases where the changing scantlings significantly affect the response. This happens for example in multi-objective optimization problems, where different Pareto optimal solutions differ considerably from each other (Romanoff et al. 2013). To take the varying hull-superstructure interaction into account, Naar et al. (2004) developed a Coupled Beam (CB) method for analysing the response of a modern passenger ship. The method is based on an assumption that each deck in the superstructure can be considered as a thin-walled beam, which are connected to each other with springs modelling the vertical and shear stiffness. CB-theory was applied in optimization process by Klanac et al. (2009) and Romanoff et al. (2013). However, it has three limitations which make it applicable only in very early design phases. First, the accurate consideration of structural discontinuity is challenge for CB-method. Second, the secondary effects of transverse bulkheads on global shear response are not considered. In addition, the shear stress is calculated at the couplings of the beams as the average shear stress of the panel.

Despite the significant development of the beam theories, the 3D Finite Element (FE) analysis is considered as the most accurate method for evaluating the passenger ship structural behaviour (ISSC 1997; DNV-GL, 2016). Structural optimization using 3D fine mesh FE-models are widely used in mass production industries such as cars (e.g. Marklund and Nilsson 2001, Duddeck 2008) and topology optimisation of load-carrying members (e.g. Duysinx and Bendsoe, 1998; Bendsoe and Sigmund, 1999; Burger and Stainko, 2006; Bruggi, 2008). However, it is computationally very expensive. The product development budgets of ships are very limited and therefore the fine mesh FE-models are only utilized in small-scale problems in later stages of design process. For example,

Ehlers (2010) and Klanac et al. (2009) optimized the tanker side structures against collision while Ringsberg et al. (2012) optimized corrugated bulkheads. Application of larger scale optimization problem can be simplified by using surrogate (Prebeg et al. 2014) and sub-modelling techniques. Sun and Wang (2011) optimized the container ships mid-section where the displacement boundary conditions were obtained from the super-elements in the fore- and aft-sections. However, this technique is unsuitable for large passenger ships, where the sections and blocks are not identical and the response analysis has to be performed fast and flexibly as the ship's general arrangement often changes and due to complex interactions between the hull and the superstructure.

In order to reduce modelling and calculation time, the ship global FE-model is created using coarse equivalent elements, where mesh density is typically 1-2 elements per web frame. Primary stiffeners such as web frames, longitudinal and transversal girders are modelled using offset beam elements which follow the Timoshenko beam theory. Secondary stiffeners are implemented into the plate or shell element formulation so that it results in equivalent extension-stiffness and mass, see Fig. 1. Commonly, equivalent element of the stiffened panel is modelled using orthotropic plate technique (Hughes 1988, DNV-GL 2015), where the stiffeners are blended with the plating so that the element has different stiffness properties in x- and y-direction. Similar elements have been used in optimization problems in various papers e.g. Zanic et al. (2007) and Zanic et al. (2013). However, these equivalent elements consider only membrane/extension stiffness, which is sufficient for capturing the ship primary response, but not for investigating local behaviour, where bending and out-of-plane shear effects become active.

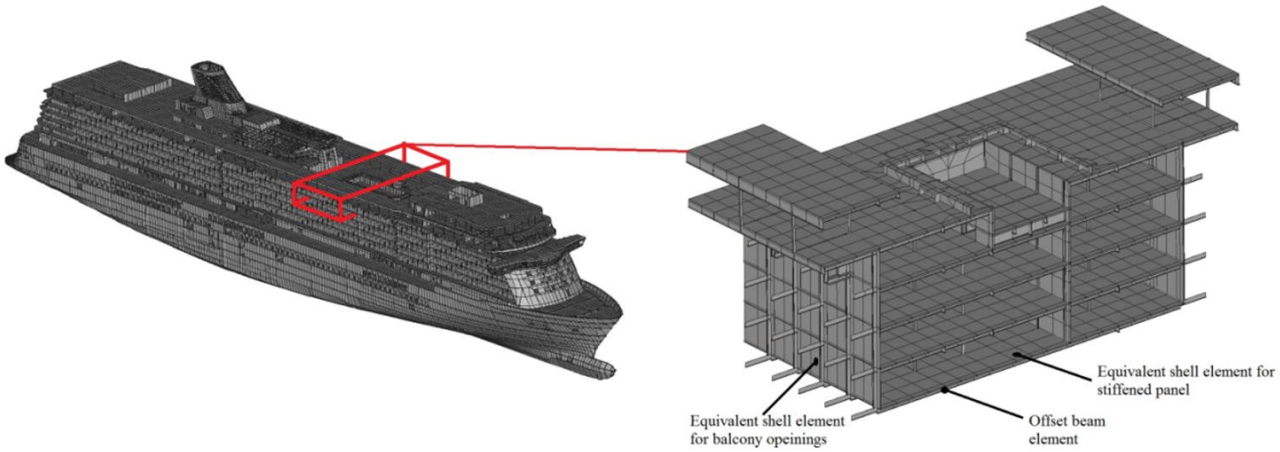


**Figure 1. Global FE model of a modern cruise ship.**

More advanced equivalent element technique was developed for web core sandwich panel by Romanoff and Varsta (2007). According to the paper the web core sandwich panel can be represented as a laminate element, which follows Equivalent Single Layer (ESL) theory (Reddy 2004). The element has also been utilized in optimization of local ship structures such as hoistable car deck (Romanoff and Klanac 2008) and steel sandwich deck in superstructure (Romanoff 2014). Avi et al. (2015) extended the ESL theory for stiffened panel, where it is described as a three layered laminate element. The first layer represents the plate, second layer represents the stiffener web and the third layer represents the stiffener flange. The element enables to change the parameters of secondary

stiffeners such as type and spacing directly from the orthotropic material properties, without re-meshing the model. This allows the optimization of wide range of materials and geometrical configurations (e.g. stiffened panels, laminates and sandwich panels).

When accurate 3D FE-models are used for optimization, singularity effects and structural discontinuities can cause local highly stressed areas. These stress concentrations are also affected by the fact that the elements are orthotropic, which leads to situations where stress concentration factors from literature are not easily applicable and direct methods are needed instead. In ship building process, these areas are separately treated in detail design phase by introducing locally thicker plates, stronger beams or insert plates, see Fig. 2. However, it is essential to already consider them in early design phase and optimization process. Despite of relevantly small area, they will dominate the scantlings for large areas and lead to over-dimensioning of the structure. In optimization literature, this issue if often treated by constraint relaxation. This means that the limiting constraint defined by design criteria is relaxed to certain degree to lead to better design instead of those limited by singularities. The criteria can be for instance stress. In ship design stress criteria is dependent on the geometry and material, limit state considered (e.g. ultimate, fatigue, serviceability, accidental) and safety margins of the structure (e.g. plastic capacity). Therefore, the amount of stress relaxation is by no means trivial task and it is not a task to be performed at conceptual design stage where design space is explored. Instead the area-ratio of plated structures with violated constrains is more informative at early design stages.

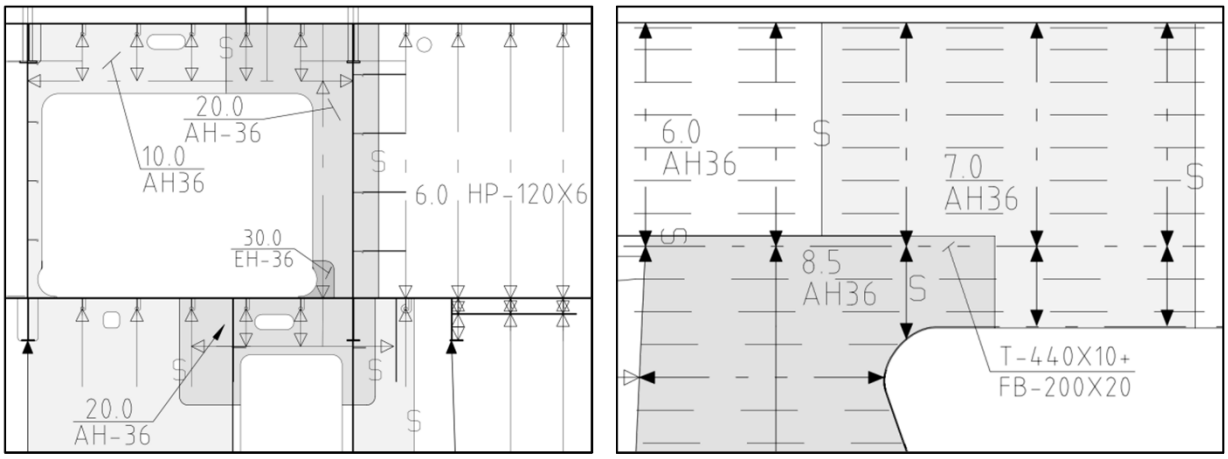


**Figure 2. Local strengthening in bulkhead (left figure) and in sun deck (right figure).**

Therefore, this paper investigates how the amount of criteria-violating elements influences the optimization result. First, we develop an advanced optimization method suitable for passenger ship structures in concept design stage. The ship's global response is obtained from the coarse mesh global FE-model based on equivalent single layer plate and corresponding beam elements, (Avi et al., 2015). Strength criteria are defined according to DNV (2014). Optimization is performed using Particle Swarm Optimization (PSO) by Kennedy & Eberhart (1995). The method should be able to distinguish between global and local strength problems and therefore, certain amount of elements can be allowed to exceed criteria.

## 2. Methods

### *2.1.Response*

Primary stiffeners such as girders and web frames are explicitly modelled using offset beam elements

due to their large participation in overall stiffness of the ship structure. NX Nastran's CBEAM element is used, which includes extension, torsion, bending in two perpendicular planes and out-of-plane shear response. Element's membrane $[A]$, membrane-bending $[B]$, and bending $[D]$ stiffnesses can be described with following matrix forms for neutral axis and for reference axis formulations (multiplication with $d_{offs}$):

$$[ABD] = \begin{bmatrix} [A] & [0] \\ [0] & [D] \end{bmatrix}$$

$$[ABD'] = \begin{bmatrix} 1 & 0 \\ d_{offs} & 1 \end{bmatrix} \begin{bmatrix} [A] & [0] \\ [0] & [D] \end{bmatrix} \begin{bmatrix} 1 & d_{offs} \\ 0 & 1 \end{bmatrix} = \begin{bmatrix} [A] & [A]d_{offs} \\ [A]d_{offs} & [D] + [A]d_{offs}^2 \end{bmatrix}, \quad (1)$$

where $d_{offs}$ is offset from beam reference-plane to the laminate element reference plane, see Fig. 3.

Secondary stiffeners with plating are modelled using equivalent single layer (ESL) theory, as presented by Avi et al (2015). The element captures the behaviour of the panel by adopting correct stiffness properties for membrane, membrane-bending, bending, in-plane and out-of-plane shear. According to the theory, a stiffened panel is modelled with three-layered laminate element. Plate layer has the thickness of the plate $t_p$, web layer thickness is equal to the height of the stiffener web $h_w$ and the flange layer has the height equal to the stiffener flange $h_f$. The cross section of the HP stiffener is idealized so that the cross sectional properties of the idealized stiffened panel matches the original stiffened panel. In order to properly capture the stiffness couplings and mass distribution between stiffened panel and T-girder, the reference plane of the laminate element is offset to top of the deck plate as shown in Fig. 3.

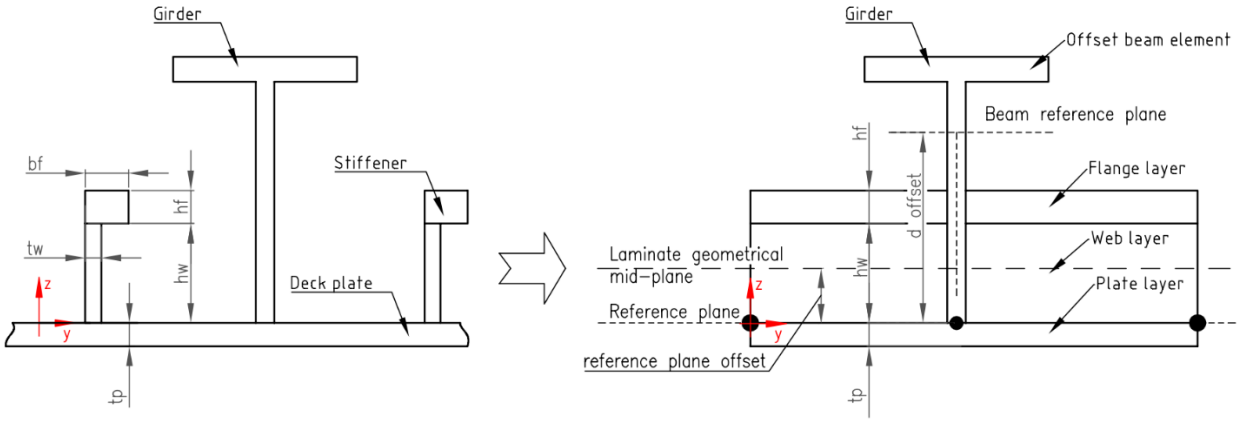


**Figure 3. Stiffened panel division into three layer laminate element and the notations used in this paper.**

According to Avi et al. (2015), relationship between homogenized internal forces and strains and curvatures can be summarized in a single matrix form:

$$\begin{Bmatrix} \{N\} \\ \{M\} \\ \{Q\} \end{Bmatrix} = \begin{bmatrix} [A] & [B] & [0] \\ [B] & [D] & [0] \\ [0] & [0] & [D_Q] \end{bmatrix} \begin{Bmatrix} \{\varepsilon\} \\ \{\kappa\} \\ \{\gamma\} \end{Bmatrix}, \quad (2)$$

where membrane $[A]$, membrane-bending $[B]$, and bending $[D]$ stiffness matrices for stiffened panel are obtained from following relations:

$$[A] = \int_{-tp}^{0} [E]_p \, dz + \int_{0}^{hw} [E]_w \, dz + \int_{hw}^{hw+hf} [E]_f \, dz \quad (3)$$

$$[B] = \int_{-tp}^{0} [E]_p \, z\mathrm{d}z + \int_{0}^{hw} [E]_w \, z\mathrm{d}z + \int_{hw}^{hw+hf} [E]_f \, z\mathrm{d}z \quad (4)$$

$$[D] = \int_{-tp}^{0} [E]_p \, z^2\mathrm{d}z + \int_{0}^{hw} [E]_w \, z^2\mathrm{d}z + \int_{hw}^{hw+hf} [E]_f \, z^2\mathrm{d}z \quad (5)$$

The plate layer is described by the elasticity matrix:

$$[E]_p = \frac{1}{(1-\nu^2)} \begin{bmatrix} E & \nu E & 0 \\ \nu E & E & 0 \\ 0 & 0 & G(1-\nu^2) \end{bmatrix}, \quad (6)$$

where $E$ is the Young's modulus, $G$ is the shear modulus and $\nu$ is the Poisson's ratio. The web and flange layers with elasticity matrixes ($[E]_w$ and $[E]_f$):

$$[E]_w = \frac{t_w}{s} \begin{bmatrix} E & 0 & 0 \\ 0 & 0 & 0 \\ 0 & 0 & 0 \end{bmatrix}, \qquad [E]_f = \frac{b_f}{s} \begin{bmatrix} E & 0 & 0 \\ 0 & 0 & 0 \\ 0 & 0 & 0 \end{bmatrix}, \quad (7)$$

where $s$ is stiffener spacing and the Rule of Mixtures have been applied.

The out-of-plane shear stiffness matrix $[D_Q]$ contains the shear stiffness in stiffener direction $D_{Qx}$ and transverse to stiffener direction $D_{Qy}$:

$$[D_Q] = \begin{bmatrix} D_{Qx} & 0 \\ 0 & D_{Qy} \end{bmatrix}, D_{Qx} = k_{xz}(G_p t_p + G_w h_w + G_f h_f), D_{Qy} = k_{yz}(G_p t_p), \quad (8)$$

where $G_p$ is the shear modulus for the plate layer and $G_w$ and $G_f$ are the shear moduli for web and flange layers, respectively. These can be obtained from the rule of mixtures as in Eq. 7. $k_{xz}$ is the shear correction factor in the $xz$-plane, which relates the maximum shear stress $(\tau_{xz})_{max}$, i.e., the shear stress at the centroid of the cross section, to the average shear stress $(\tau_{xz})_{avg}$ (Avi et al. 2015). The shear correction factor $k_{yz}$ = 5/6 is derived from the plate shear energy and is included in Reissner-Mindlin plate theory (Whitney and Pagano 1970).

In result evaluation, the obtained normal and shear stresses from laminate element web and flange layer need to be scaled by localisation which transforms the volume averaged stress of structural members and voids back to that of structural components using following relations:

$$\sigma_{w,actual} = \frac{s}{t_w}\sigma_w, \sigma_{f,actual} = \frac{s}{b_f}\sigma_f, \tau_{w,actual} = \frac{s}{t_w}\tau_w, \tau_{f,actual} = \frac{s}{b_f}\tau_f. \quad (9)$$

If lateral loads are included in optimization process, an additional plate bending between the stiffeners occurs as it shown in Fig 4. This cannot be captured by the homogenized ESL model as the actual periodic structure is smeared to continuum. Avi et al. (2015) showed that this local response can be considered by using superposition principle:

$$\begin{Bmatrix} \sigma_x^{tot} \\ \sigma_y^{tot} \\ \tau_{xy}^{tot} \end{Bmatrix}_i = \begin{Bmatrix} \sigma_x^{g} \\ \sigma_y^{g} \\ \tau_{xy}^{g} \end{Bmatrix}_i + \begin{Bmatrix} \sigma_x^{l} \\ \sigma_y^{l} \\ \tau_{xy}^{l} \end{Bmatrix}_i, i = t, b \quad (10)$$

where subscripts t and b denote top and bottom surface, respectively, and superscripts $g$ and $l$ denote the global (ESL) and local response, respectively. Similar principle can be used to obtain the total deflection of plating.

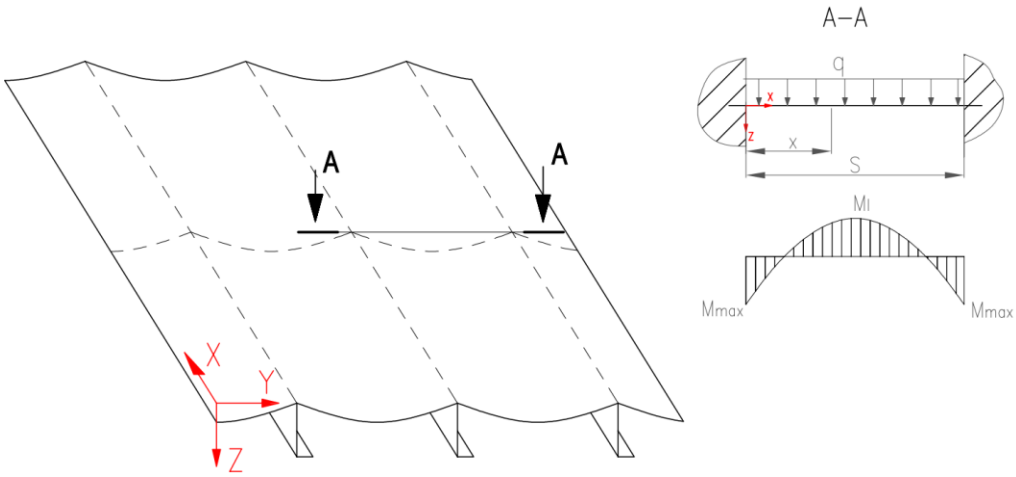


**Figure 4. Local plate bending between the stiffeners (Avi et al. 2015).**

### *2.2. Optimization*

In this paper a Particle Swarm Optimization (PSO) algorithm from (Jalkanen 2006) is used. PSO is initialized from a set of design alternatives i.e. initial population, which is updated in every generation by two parameters: previous position and velocity. The new position of each particle can be obtained from following formula:

$$\boldsymbol{x}_{k+1}^{i} = \boldsymbol{x}_{k}^{i} + \boldsymbol{v}_{k+1}^{i}, \tag{11}$$

where $\boldsymbol{x}_{k}^{i}$ is a vector containing current position of particle $i$ and $\boldsymbol{v}_{k+1}^{i}$ is a vector containing velocity of particle $i$ in iteration round $k+1$. Velocity is calculated from:

$$\boldsymbol{v}_{k+1}^{i} = w\boldsymbol{v}_{k}^{i} + c_1 r_1\left(\boldsymbol{p}_{k}^{i} - \boldsymbol{x}_{k}^{i}\right) + c_2 r_2\left(\boldsymbol{p}_{k}^{g} - \boldsymbol{x}_{k}^{i}\right), \tag{12}$$

where $\boldsymbol{p}_{k}^{i}$ is the best-known location of particle $i$ and $\boldsymbol{p}_{k}^{g}$ is the best known location of the entire swarm at given iteration round $k$. The parameter $w$ is called inertia and terms $c_1$ and $c_2$ are called cognitive and social parameters, which are typically chosen between 0 and 2. Terms $r_1$ and $r_2$ are uniformly distributed random numbers between 0 and 1. The inertia term $w\boldsymbol{v}_{k}^{i}$ is guiding the search into wider area of design space while terms including $\boldsymbol{p}_{k}^{i}$ and $\boldsymbol{p}_{k}^{g}$ direct it towards promising solution, see Fig. 5.

In PSO, the constraints are taken into account by a penalty factor. It is given for each design alternative which violates the constraints. The objective function depends on how much the constraint is violated and it is described by the following formula:

$$F(x)\left[1 + \sum_{g_j(x)>0} \lambda g_i(x)\right], \tag{13}$$

where $\lambda$ is the penalty factor. If the penalty factor is chosen too small, too many of the design alternatives become unsatisfied and when the factor is too large, good alternatives, which violate the constraints only by little are ruled out.

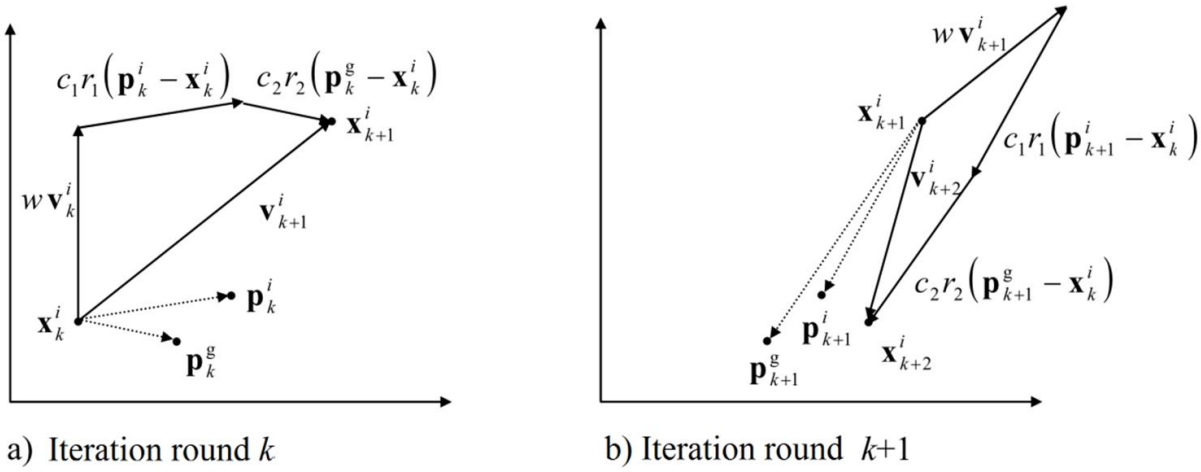


**Figure 5. Iteration steps of PSO, a) iteration step from $x_k^i$ to $x_{k+1}^i$ b) iteration step from $x_{k+1}^i$ to $x_{k+2}^i$ (Jalkanen 2006).**

## 3. Implementation

### *3.1. Optimization platform*

The optimization process is carried out with a user-defined Matlab-routine which links together the FE-model creation, response and strength evaluation and PSO algorithm. The models are created and analysed using commercial FE software FEMAP with NX Nastran. Flowchart of the optimization process is presented in Fig. 6.

The process starts with setting the design variables $[x]$ and their limits, defined as:

$$[x] = \left[\left\{x_{panel,1}, \dots, x_{panel,N}, x_{girder,1}, \dots, x_{girder,N}\right\}\right] \qquad (14)$$

The matrix $[x]$ contains sub-design vectors of all stiffened panel groups, $\{x_{panel,i}\}$, and for all girder groups, $\{x_{girder,i}\}$. The stiffened panel vector contains variables for plate thickness, stiffener size, stiffener spacing, length of the panel as well as Young's modulus, density, yield strength and Poisson's ratio separately for plate, stiffener web and stiffener flange. Similarly the design vector for girders consists of web thickness and height, flange thickness and width, Young's modulus, yield strength and Poisson's ratio. Each of these variables can be constrained to have same value between multiple sub-design vectors, i.e. optimization groups. This will reduce the number of variables in the optimization problem and constrain the FE-model scantlings. From the design variables the initial population i.e. the new design alternatives (DA) are produced. For each sub-vectors critical constraint values are calculated (Appendix A) and for each design alternative an input file is generated in order to carry out the analysis. From the calculated stresses, the designs are checked with respect to strength criteria formulated as:

$$g(x) = \frac{\sigma_a}{\sigma_{cr}} - 1, \qquad (15)$$

where $\sigma_a$ is stress on element and $\sigma_{cr}$ is the critical stress in respect to constraints.

The objective function is obtained from FE-analysis output file. The maximum constraint value and the objective function value are sent to optimization algorithm where the next set of design alternatives is evaluated.

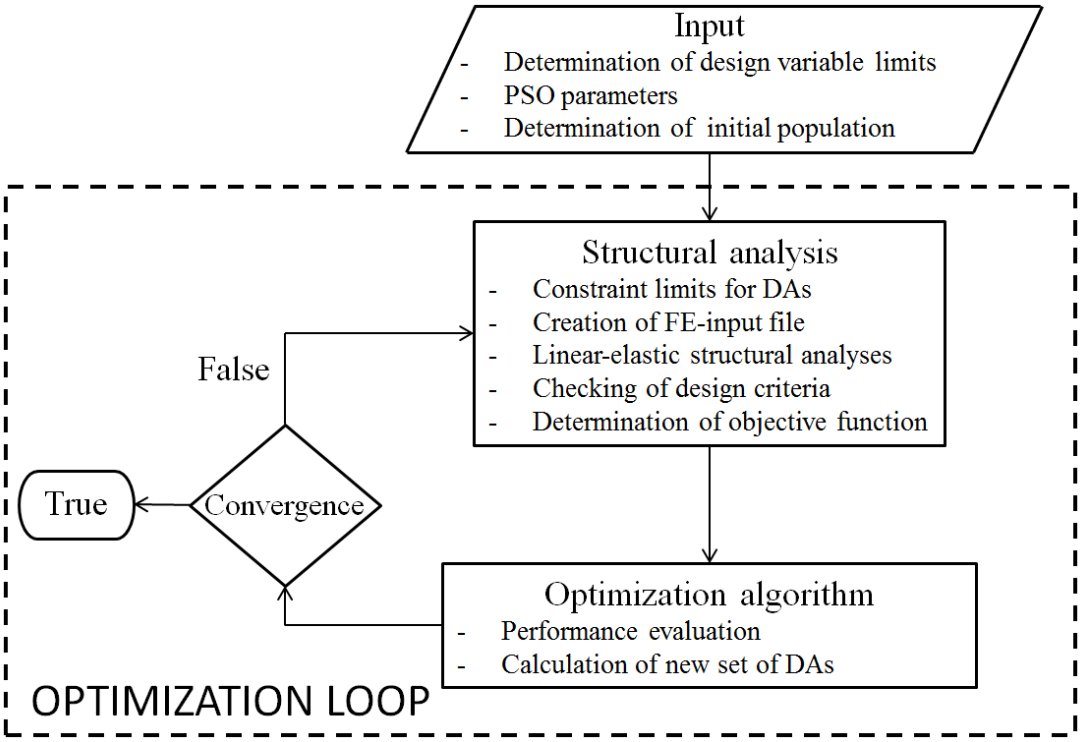


**Figure 6. Flow chart of the optimization process.**

### *3.2. Local strength problems and indirect constrain relaxation*

Local strength problems are arising in the global FE-model in way of structural discontinuities or openings in decks and bulkheads. These discontinuities are introduced by functional and architectural requirements and are considered here as input for structural design. As the stiffened panels are orthotropic and hull girder load carrying mechanism complex, the magnitude of stress concentration around these discontinuities is difficult to assess prior the FE-analysis is carried out. In addition, in practice these are usually treated after concept design phase with local reinforcement, Fig. 2. For example, higher plate thicknesses for opening corners or intermediate stiffeners in buckling critical areas. The high stresses can violate constraints and increase the scantlings of entire panel or girder group, leading to larger structural weight than actually needed. In this work the local strength problem is treated by allowing certain ratio of elements to violate constraint and by optimizing the structure for this fixed ratio. Thus, instead of relaxing the constraints directly at Eq. (15) by increasing the allowed stress levels, we only take certain elements to the constraint evaluation. This idea originates from the basic design and production processes where local strengthening must be assessed with more accurate design methods and decisions to the implementation into production and operation must be carried out. In the beginning of optimization, a certain percentage of area of stiffened panel and a certain percentage of elements of primary girders are defined, which can violate constraints in the optimization group. Later, these local scantlings of violated areas are separately defined.

### *3.3. Classification of constrain types for different element groups*

From optimization point of view here we divide the elements into 5 types, see Table 1. Firstly, either all (type 1) or selected (type 2) constraints are evaluated and scantlings are changed in the optimization process and secondly, the scantlings are kept constant during the optimization process, types 3-5, with all/selected/none constrains evaluated respectively. This makes it possible to optimize

only part of the model and is beneficial in optimization of large complex structure, where some part of the structure is defined using classification rules and some locations will be later separately defined using special load cases and local models. The approach enables to consider special cases. For example, T-girders typically belong to element type 3 or 4, as their scantlings are defined based on vibration results and outfitting requirements, while it is still important to satisfy global strength criteria. Type 5 elements could be such additional structures that are already included in the global FE-model, but their actual design will be done later and optimization is therefore irrelevant. Good example might be sundeck structures or helideck.

**Table 1. Types of optimized elements**

| | | Scantlings changed | | | |
|---|---|---|---|---|---|
| | | Yes | Classification description | No | Classification description |
| Constraints evaluated | All | type 1 | Optimized structures | type 3 | Structures which carry global loads but dimensioning comes from other design factors, e.g. T-girders |
| | Selected | type 2 | Optimized structures where some constraints are limiting the scantlings, e.g. stress criteria for opening corners | type 4 | Structures which carry global loads but dimensioning comes from other design factors, e.g. architectural roof structures where comfort criteria is not important |
| | | | | type 5 | Special structures where dimensioning doesn't come from applied global loads, e.g. architectural sundeck structures or helideck |

## 4. Case study

### *4.1. Case definition*

Applicability of the optimization method for large complex structure is tested on the main frame of a modern cruise ship. The ship length between perpendiculars is $L_{pp}$=286.944 m, breadth $B$=35.8 m and draught $T$=8.05 m. She has 13 decks with total height of 43.7 m. The frame and web frame spacing are 854 mm and 2562 mm, respectively. Fire bulkheads, which are not optimized, type 5 in Table 2, are located at every 40.992 m. They are made of 6 mm plate, which is stiffened using HP-120x6 profiles and girders T-250x8+150x10. The ship is made of two types of steel: NV-NS and NV36, with yield strengths of 235 MPa and 355 MPa, respectively. For both materials Young's modulus is 206 GPa and Poisson ratio is 0.3. The main frame drawing with scantlings kept constant during the optimization process as well as optimization groups are presented in Fig. 7.

The ship is idealized as a prismatic beam and only the quarter of the structure is modelled due to symmetry, Fig. 8. Girders, frames and pillars are modelled using offset beam elements (CBEAM). Plating with secondary stiffeners are expressed using laminated shell elements (CQUAD4), which follow the ESL theory presented in Avi et al. (2015). General mesh density is two elements per web frame spacing and 3-4 elements per deck height, which is sufficient to capture the hull global behaviour correctly (Avi et al. 2015). Denser mesh is used around the sideshell openings between deck 3 to 5. The model includes 30379 laminate and 17348 beam elements, which means 176610 degrees of freedom (DOF).

Vertical bending moments are considered and calculated using classification society rules, DNV (2014). The ship maximum bending moments due to hogging and sagging loading condition

are 7.343*106 kNm and -4.616*106 kNm, respectively. The moments are generated by applying cosine shape pressure on the ship bottom elements, see Fig. 9:

$$p = p_{max} \cos\left(\frac{x\pi}{0.5L}\right), \tag{16}$$

where maximum pressure $p_{max}$ for hogging and sagging condition are 49.2 kPa and -30.94 kPa respectively. This type of loading will create highest moment at the midship and highest shear forces at position L/4 and 3L/4.

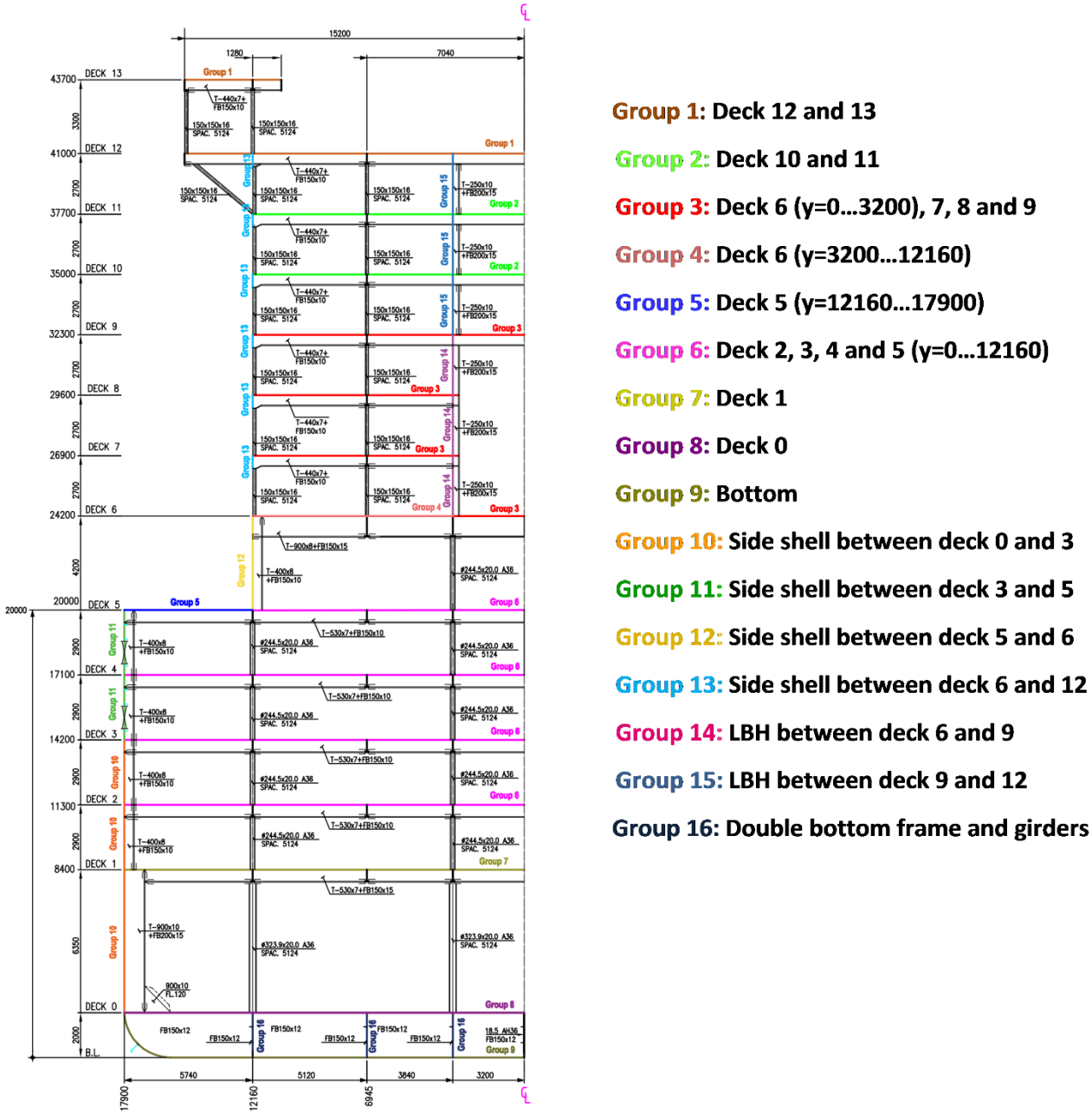


**Figure 7. Main frame drawing with scantlings kept constant during optimization process (left) and optimization groups (right)**

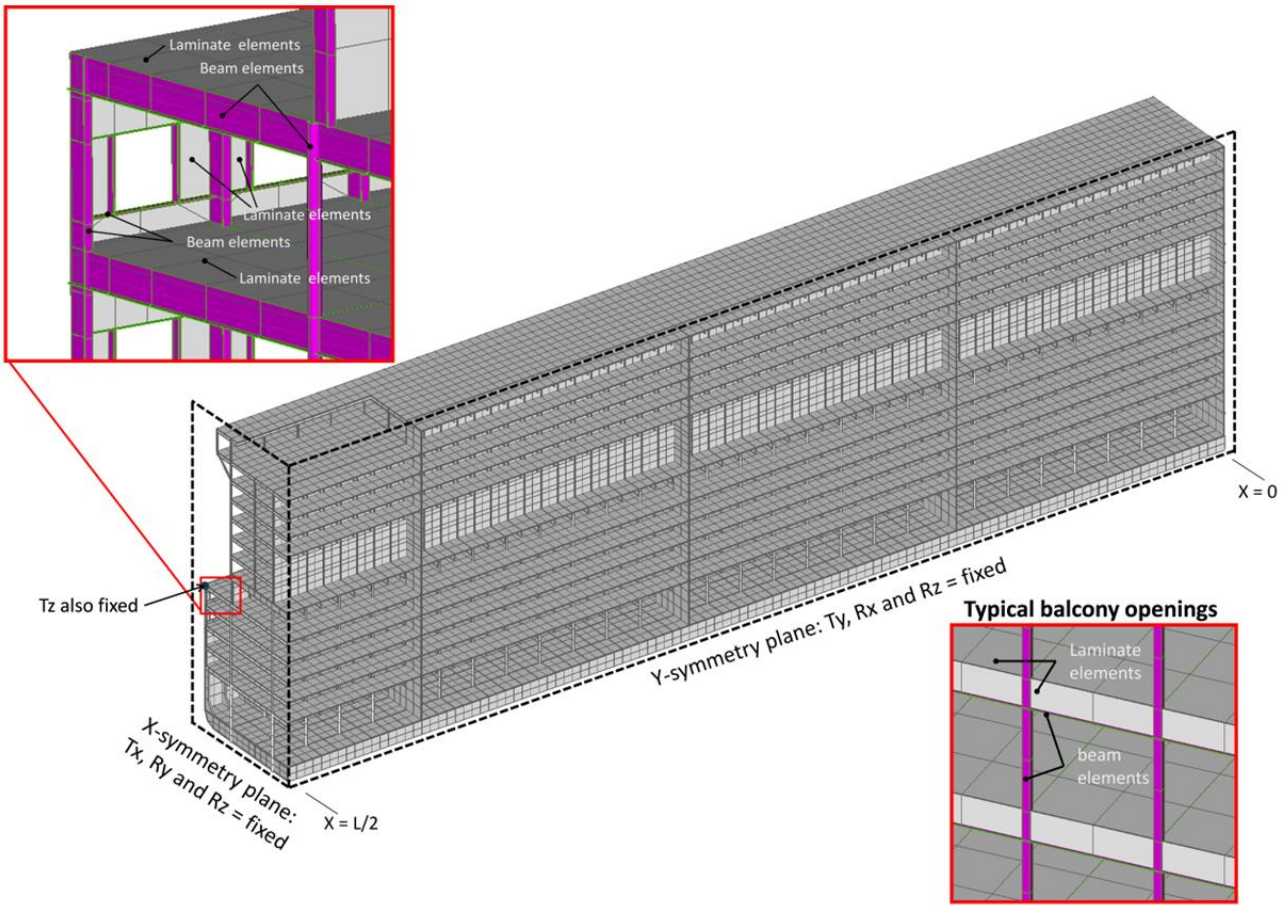


**Figure 8. Prismatic FE-model of modern cruise ship.**

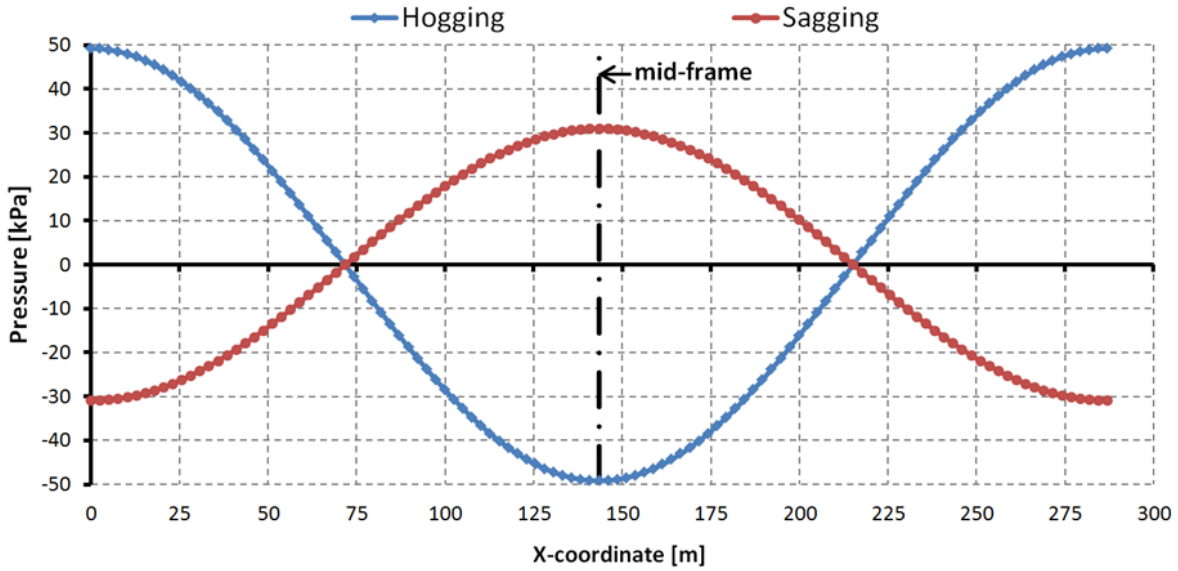


**Figure 9. Loading for the prismatic ship bottom structure.**

### *4.2. Optimization*

The optimized groups are illustrated in Fig. 7 and their design variables are given in Table 2. Stiffener spacing for superstructure decks (groups 1-4), main hull decks (groups 5-9) and longitudinal bulkheads (groups 15-16) are constrained to be equal for keeping optimized solution production friendly. T-girders are typically limited by vibration and deck height criteria and therefore their scantlings are kept constant in the optimization process. Also the pillars remain the same. The model is optimized using buckling and yielding constraints for laminate elements and only yielding constraints for beam elements, see Appendix A.

Optimization is performed with the swarm size of 20 and the analysis is run for 75 iterations, leading to 1500 design alternatives. The penalty factor is set to 1.5 for infeasible solutions. Inertia term is set to 1.4 and parameters $c_1$ and $c_2$ are set to 2. Objective of the optimization is to reduce mass.

Optimization is performed for 3 separate cases by allowing maximum of 1%, 5% and 10% of constraint violation in each optimization group for each load case. In stiffened panel groups this means percentage of area that can violate constraint, while in girder groups it means percentage of number of elements which can exceed criteria. After optimization, the local reinforcements for violated areas are applied according to common shipyard practice. For example, if buckling criteria is exceeded in small area, buckling stiffeners are added. If buckling or yielding criteria is exceeded in larger area, the plate thickness is increased.

**Table 2. Design variables for optimization groups**

| Group | Structure | Plate thickness [mm][a] | Stiffener size | Stiffener spacing [mm] |
|---|---|---|---|---|
| 1 | Superstructure decks | 7.0-10.0, 12.0 | HP-100x6, HP-120x6, HP-140x7 | 515, 575, 645, 740[b] |
| 2 | | 5.0-7.0 | HP-100x6, HP-120x6, HP-140x7 | |
| 3 | | 5.0-6.5 | HP-80x5, HP-100x6, HP-120x6 | |
| 4 | | 7.0-10.0 | HP-80x5, HP-100x6, HP-120x6 | |
| 5 | Hull decks & double bottom | 8.0, 9.0-12.0 | HP-100x6, HP-120x6 | 515, 575, 645, 740[c] |
| 6 | | 5.0-6.5 | HP-80x5, HP-100x6, HP-120x6 | |
| 7 | | 5.0-6.5 | HP-80x5, HP-100x6, HP-120x6 | |
| 8 | | 10.0-15.0 | HP-160x7, HP-180x8 | |
| 9 | | 14.0-18.0 | HP-200x9, HP-220x10, HP-240x10, HP-260x10 | |
| 10 | Side shell | 10.0-15.0 | HP-160x8, HP-180x8 | 530, 580, 635, 705[d] |
| 11 | | 12.0-18.0 | HP-160x7 | |
| 12 | | 8.0-13.0 | HP-120x6, HP-140x7 | 530, 580, 635, 705 |
| 13 | | 14.0-17.0 | - | - |
| 14 | Superstructure longitudinal bulkhead | 7.0-10.0 | HP-100x6, HP-120x6 | 540, 600, 675 [e] |
| 15 | | 7.0-10.0 | HP-100x6, HP-120x6 | |
| 16 | Double bottom frame & girders | 11.0-15.0 | FB-150x12 | 685 |

[a] the increment of plate thickness is 0.5 mm from 5-9 mm and 1.0 mm from 9-18 mm

[b] same stiffener spacing is constrained for groups 1, 2, 3 and 4

[c] same stiffener spacing is constrained for groups 5, 6, 7, 8 and 9

[d] same stiffener spacing is constrained for groups 10 and 11

[e] same stiffener spacing is constrained for groups 14 and 15

### *4.3.Results*

Development of the objective function for each optimization case, where 1, 5 or 10% of constraint violation is allowed, is shown in Fig. 10. Optimum designs for each case are presented in Table 3. As expected, the minimum solution, i.e. mass, is found with the 10% case, but the biggest difference can be seen between 1% and 5%, see also Table 4. When the 1%, 5% and 10% cases were corrected manually to be feasible, the difference in total mass did not change significantly, i.e. the benefit of the approach remains with 6-7.6% of smaller mass compared to the case where only 1% of constraint violation is allowed.

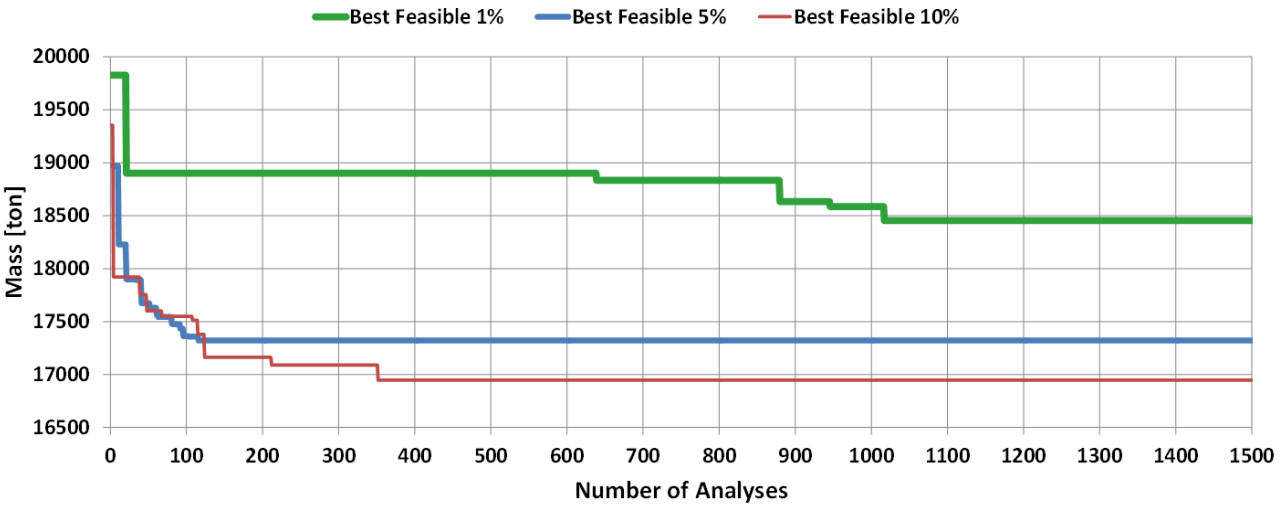


**Figure 10. Convergence of objective function.**

**Table 3. Optimum design for cases where 1, 5 and 10% of constraint violation is allowed**

| Group | Optimum design | | | | | | | | |
|---|---|---|---|---|---|---|---|---|---|
| | Thickness [mm] | | | Spacing [mm] | | | Stiffener type | | |
| | 1% | 5% | 10% | 1% | 5% | 10% | 1% | 5% | 10% |
| Group 1: Deck 12 and 13 | 8.0 | 7.0 | 7.0 | 515 | 515 | 515 | HP-140x7 | HP-100x6 | HP-100x6 |
| Group 2: Deck 10 and 11 | 7.0 | 7.0 | 5.5 | 515 | 515 | 515 | HP-140x7 | HP-100x6 | HP-140x7 |
| Group 3: Deck 6 (y=0…3200), 7, 8 and 9 | 5.0 | 5.0 | 5.0 | 515 | 515 | 515 | HP-80x5 | HP-80x5 | HP-80x5 |
| Group 4: Deck 6 (y=3200…12160) | 10.0 | 10.0 | 10.0 | 515 | 515 | 515 | HP-80x5 | HP-80x5 | HP-120x6 |
| Group 5: Deck 5 (y=12160…17900) | 8.0 | 12.0 | 12.0 | 515 | 515 | 740 | HP-100x6 | HP-100x6 | HP-100x6 |
| Group 6: Deck 2, 3, 4 and 5 (y=0…12160) | 5.5 | 5.0 | 5.0 | 515 | 515 | 740 | HP-80x5 | HP-80x5 | HP-80x5 |
| Group 7: Deck 1 | 6.5 | 6.5 | 6.5 | 515 | 515 | 740 | HP-80x5 | HP-80x5 | HP-120x6 |
| Group 8: Deck 0 | 10.0 | 10.0 | 10.0 | 515 | 515 | 740 | HP-180x8 | HP-160x7 | HP-160x7 |
| Group 9: Bottom | 14.0 | 14.0 | 14.0 | 515 | 515 | 740 | HP-260x10 | HP-200x9 | HP-200x9 |
| Group 10: Side shell between deck 0 and 3 | 15.0 | 10.0 | 10.0 | 530 | 530 | 530 | HP-160x8 | HP-160x8 | HP-160x8 |
| Group 11: Side shell between deck 3 and 5 | 18.0 | 12.0 | 12.0 | 530 | 530 | 530 | HP-160x7 | HP-160x7 | HP-160x7 |
| Group 12: Side shell between deck 5 and 6 | 13.0 | 13.0 | 13.0 | 530 | 705 | 530 | HP-120x6 | HP-120x6 | HP-120x6 |
| Group 13: Side shell between deck 6 and 12 | 17.0 | 14.0 | 14.0 | - | - | - | - | - | - |
| Group 14: LBH between deck 6 and 9 | 10.0 | 7.0 | 10.0 | 540 | 540 | 675 | HP-100x6 | HP-100x6 | HP-120x6 |
| Group 15: LBH between deck 9 and 12 | 7.0 | 10.0 | 7.0 | 540 | 540 | 675 | HP-120x6 | HP-120x6 | HP-120x6 |
| Group 16: Double bottom frame and girders | 11.0 | 11.0 | 11.0 | 685 | 685 | 685 | FB 150x12 | FB 150x12 | FB 150x12 |

**Table 4. Total ship mass after optimization and after adding additional local strengthening**

| Optimization case | After optimization | | After adding local strengthening | | |
|---|---|---|---|---|---|
| | Total mass [t] | Difference between 1% | Total mass [t] | Mass increase [t] | Difference between 1% |
| 1 % | 18454 | 100 | 18463 | 9 | 100 |
| 5 % | 17321 | 93.9 | 17350 | 29 | 94.0 |
| 10 % | 16946 | 91.8 | 17064 | 118 | 92.4 |

Hull girder deflection after optimization as well as after local strengthening is presented in Table 5. As expected, lighter design results in larger deflection, while local strengthening does not decrease the global deflection noticeably. The difference in deflection between 1 and 5% case is approximately 10%, and between 1 and 10% case about 11%. The load-carrying mechanism stays very similar between difference cases, see X-directional axial force and shear flow distributions in Fig. 11.

X-normal stress in deck plating of optimized and locally strengthened structure for 1% and 10% case is shown in Fig. 12. Variation along deck is shown with markers and average value is used to draw the distribution in *z*-direction. Variation in stress is the largest at the location of discontinuity between hull and superstructure, i.e. shear lag area at decks 5 and 6. Stress distribution is complex and does not follow classical beam theory. Thus, using more advanced methods for optimization, such as global FE-analysis with ESL element, is justified.

**Table 5. Hull girder deflection after optimization and after additional local strengthening**

| Optimization case (% of allowable constraint violation) | After optimization | | After local strengthening | |
|---|---|---|---|---|
| | Hogging, max dz [mm] | Sagging, max dz [mm] | Hogging, max dz [mm] | Sagging, max dz [mm] |
| 1 % | 390 | 245 | 389 | 243 |
| 5 % | 432 | 273 | 429 | 270 |
| 10 % | 440 | 278 | 432 | 272 |

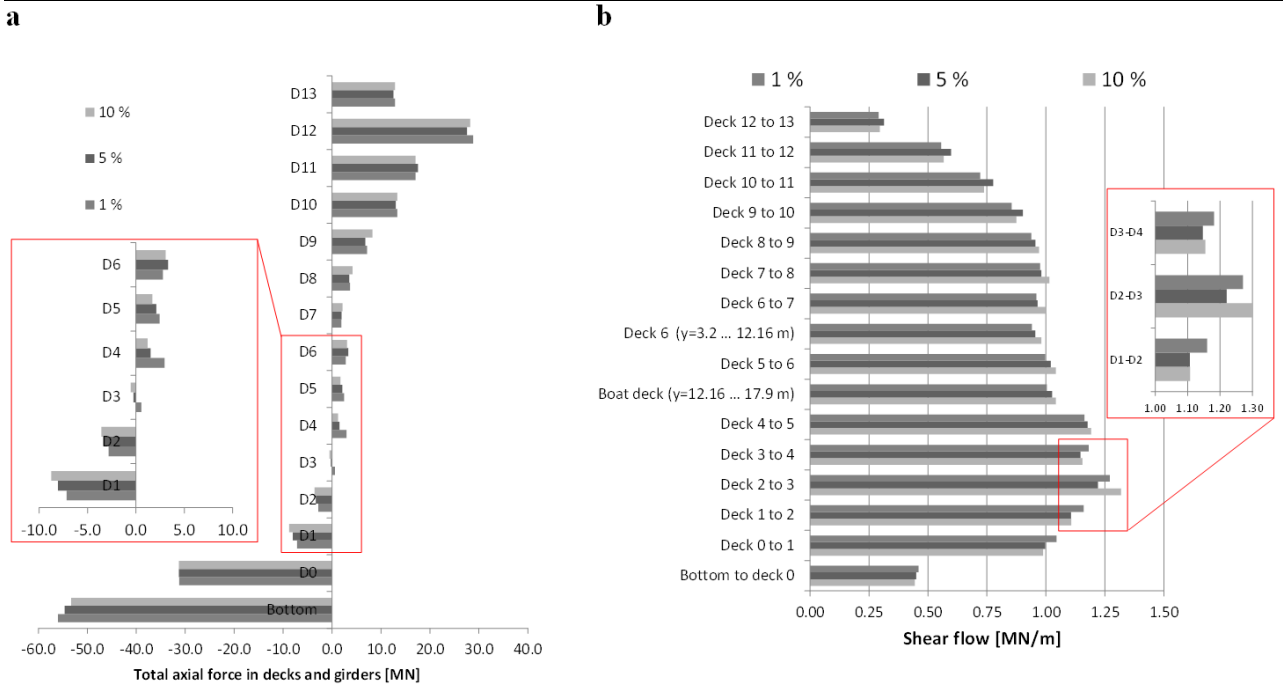


**Figure 11. (a) Total X-directional axial force at L/2 and (b) Shear flow at L/4.**

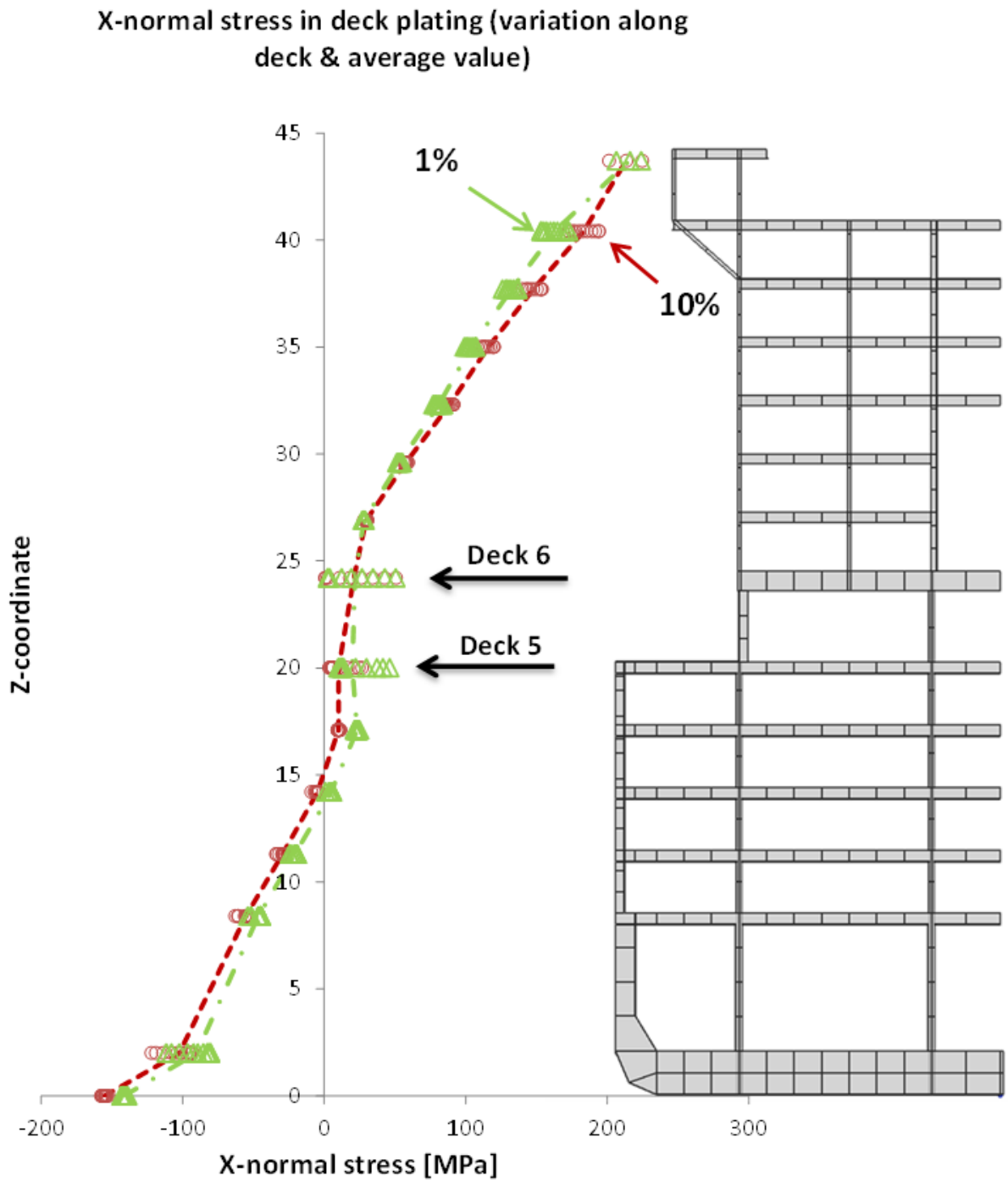


**Figure 12. X-normal stress in deck plating (variation along deck as well as average value) for optimized structure with local strengthening at L/2; 2 cases where 1 or 10% of constraint violation is allowed.**

As seen from Fig. 12, the highest stresses occur at the upmost continuous deck of superstructure. This deck often has large cut-outs due to pools or other features, which cause locally very high stresses. If local stress concentration is not considered by letting some part of the structure violate the optimization constraint, the whole deck would result in larger plate thickness and bigger stiffeners, see also Table 3. This is an example of a location where the benefit of indirect constrain relaxation has most potential. Another example is longitudinal bulkhead which transfers the shear between the decks. In this case, the effect of indirect constraint relaxation is shown in Fig. 13 for 1%, 5% and 10% cases for longitudinal bulkhead in superstructure. Maximum usage factor for hogging and sagging

for each element is enveloped for groups 14 and 15, see Fig. 7. Elements violating any of the constraints are shown in white colour and these locations are reinforced later manually. As mentioned earlier, this adds very little weight to the structure.

The usage factor of biaxial buckling after optimization and after local strengthening is presented in Fig. 14 for all three cases. Elements violating the constraint are shown in white colour. Two main critical areas can be identified. First includes the upper decks at midship area, especially around the cut-outs at upmost deck, where X-directional stresses exceed the longitudinal buckling criteria. Second is the location of hull and superstructure connection on deck 5 and 6, where Y-directional stresses exceed the transverse buckling criteria, which for longitudinally stiffened panel is relatively low. These places are examples of locations where in design more advanced computational analyses such as non-linear FEA could be used. Also, in these areas the production quality will become important as it has direct effect to the allowed stress levels. Therefore, these types of analyses are considered to be relevant for the basic design stage. In principle it is possible to gain weight savings at this stage if the strength values are increased by proper detail design and production.

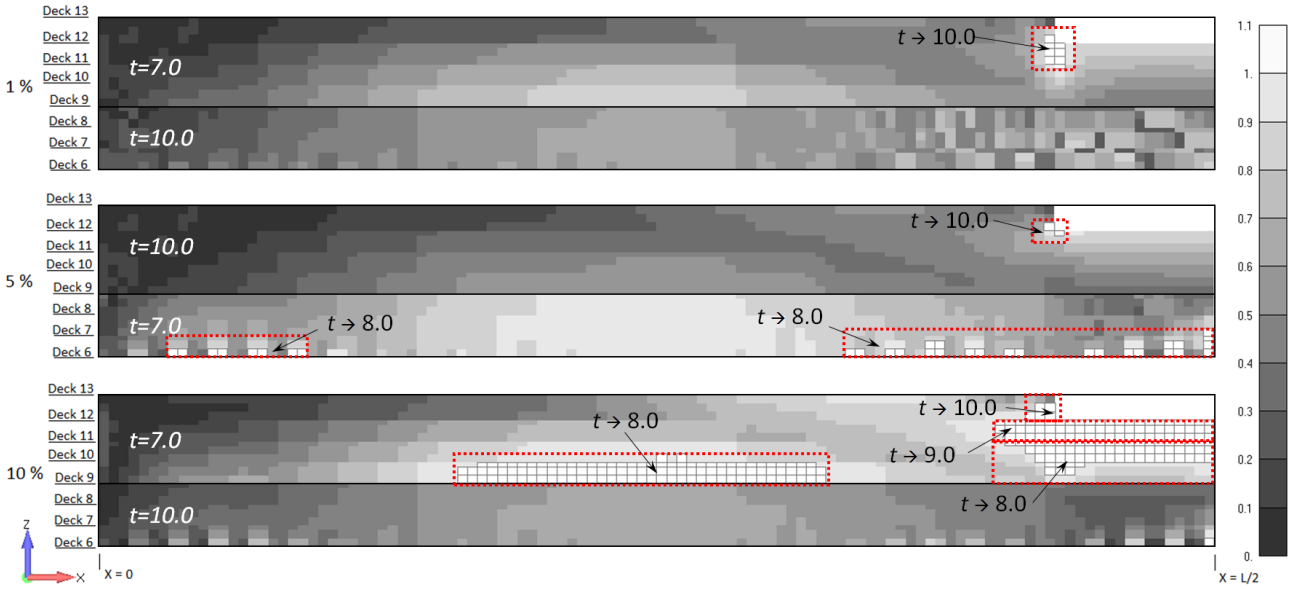


**Figure 13. Maximum usage factor for longitudinal bulkhead groups in hogging and sagging loading conditions. Elements exceeding the criteria are shown in white colour.**

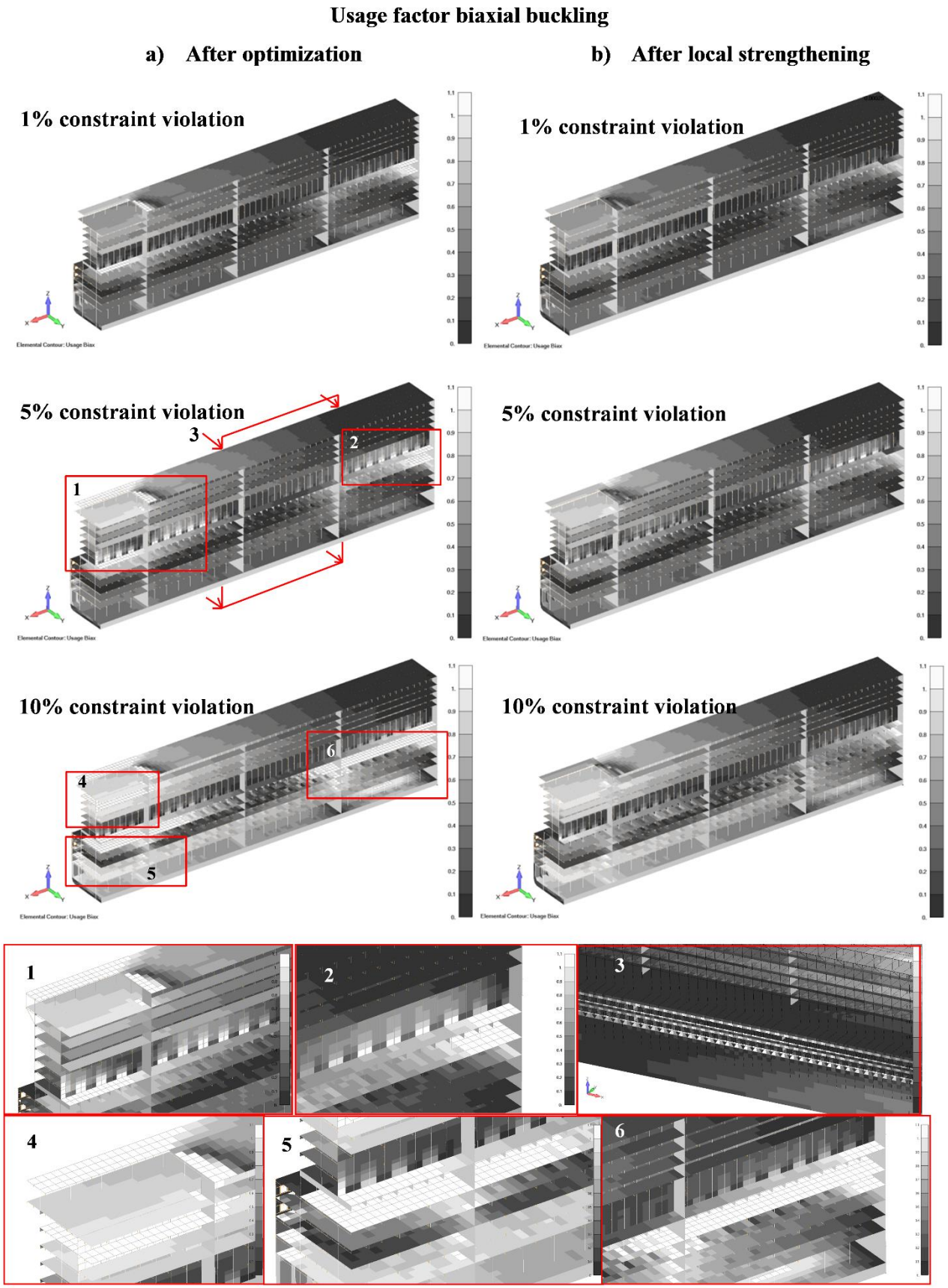


**Figure 14. Usage factor of biaxial buckling. Elements exceeding the criteria are shown with white colour. Comparison of the usage factors after optimization (a) and after local strengthening (b) shows the modified areas of the hull.**

## 5. Discussion

This paper presents the optimization method suitable for modern passenger ship utilizing global FE-analysis and ESL element. It fits for early, i.e. concept, design phases as it is possible to change the scantlings of the stiffened panel quickly from the material properties of ESL element without re-meshing the model. Structures are divided into optimization groups in order achieve production-friendly scantlings, for example same stiffener spacing for all superstructure decks, Fig. 7. Elements are additionally divided into 6 types, Table 1, which enables applying different design principles for different structures: either all, some or none of the constraints are checked and either the scantlings are changed or not based on the check. Global FE-model of a passenger ship includes lots of different structures, where some are defined based on yielding and buckling criteria only, while others may be governed by vibration restrictions, fatigue, accidental or local loads. In practice, these different limit states enter the ship design at different stages of classical design spiral due to different amount of information needed to perform reliable analysis. Some local structures are designed later and thus their inclusion in the optimization process would be irrelevant. This kind of flexibility enables efficient handling of global FE-model.

In order to achieve lightweight design, local stress peaks are handled by allowing certain area of plates, described by the amount of elements to exceed the strength criteria. In this paper, we call this process indirect constraint relaxation as instead of adjusting the constrain equation; we consider only certain elements that enter constraint evaluations. The classes of elements used in this paper, are derived from practical passenger ship design and construction process that include discussion between design and production departments on design limits and their impact to costs and building process. These high-stressed areas are later locally strengthened. In presented case study, 1, 5 and 10% of the area of the stiffened panels and of the number of elements of girders were allowed to exceed the strength criteria in hogging and sagging loading conditions. Optimum design solutions were then locally strengthened according to normal shipyard practice. The results show significant difference in achieved total mass between 1 and 5% case (1113 t), but the step from 5 to 10% is not so noticeable anymore (286 t). The obtained mass savings depends on the applied loads and boundary conditions. Using different loading conditions i.e. racking or deck pressures, the mass saving can be different in comparison to the present case study.

Even though the case study is a prismatic model of a modern passenger ship, the influence of local strength issues is still significant. Difference in total mass in final optimized and locally strengthened solution between 1 and 10% cases is 7.6%, while local strengthening decreased the difference only 0.6%. Actual global FE-model of a passenger ship includes much more bulkhead discontinuities, openings and other stress concentrations, which create lots of highly stressed local areas. If these are not considered by allowing certain amount of elements to exceed optimization criteria, the over-dimensioning can be even higher than in presented example.

In current paper only the mass was optimized and the load-carrying mechanism stayed similar between different cases of allowed constraint violation. If multi-objective optimization would be carried out, the load-carrying mechanism may also change more as was shown in Romanoff et al. (2013).

The present investigation was carried out using strength criteria from classification society rules which is current industry practice, see also for example Richir et al. (2007), Klanac et al. (2009)

& Romanoff et al. (2013). This is justified in present context as we focus on conceptual design stage where the objective is to explore the design space effectively to understand the impact of various design parameters on overall design. For the later design stages the approach could be improved by utilizing direct calculation methods for constraint checks of different limit states, by including production constrains by cost benefit analyses and architectural criteria. This is left for future work.

## 6. Conclusions

This paper presents the optimization method for passenger ship global FE-model utilizing ESL element. Based on the results, following conclusions can be drawn:

- ESL element is suitable for optimizing large complex structures such as modern passenger ships, because the layer-wise formulation of the element allows changing the scantlings of the stiffened panel without re-meshing the model.
- Due to layer-wise formulation, it is also possible to easily check the stresses in deck plate and stiffener separately, which enables efficient buckling/yield check.
- Local stress concentrations, which are usually considered later in the detail design phase, can dominate the optimization result and lead to over-dimensioned structures. By allowing certain percentage of area to violate optimization constraints and later locally strengthen these areas, it is possible to obtain much lighter design.
- Presented optimization approach divides elements into 5 types, which enables applying different design principles for different structures. This is beneficial in optimization of modern passenger ship, where not all structures are defined based on yielding and buckling criteria only.
- The method can easily be extended for multi-objective optimization to also consider the center of gravity and cost. It is also possible to add more load cases such as lateral loads, or to consider vibration as one of the constraints.

## Acknowledgements

The work was supported by the LOURA (Lounaisrannikkoyhteistyö) and Meyer Turku Oy. The financial support is gratefully appreciated.

## References

Avi E, Lillemäe I, Romanoff J, Niemelä A. 2015. Equivalent shell element for ship structural design. Ships and Offshore Struct. 20(3): 239-255.

Bendsoe, M.P. and Sigmund, O., “Material interpolation schemes in topology optimization”, Archive of Applied Mechanics, Vol 69, 1999, pp. 635-654.

Bruggi, M, “On an alternative approach to stress constraints relaxation in topology optimization”, Structural Multidisciplinary Optimization, Vol. 36, 2008, pp. 125-141.

Burger, M. and Stainko, R., “Phase-field relaxation of topology optimization with local stress constrains”, SIAM Journal of Control Optimisation, Vol. 45, No. 4, 2006, pp. 1447-1466.

Caprace J-D, Bair F, Rigo P. 2010. Least weight and least cost optimization of cruise ships. Ship Technol Res. - Schiffstechnik 57(3): 210-220.

Det Norske Veritas. 2014. Pt.3 Ch.1 Hull structural design - ships with length 100 meters and above. Høvik.

DNV-GL. 2015. Finite Element Analysis. DNVGL-CG-0127.

DNV-GL. 2016. Direct strength analysis of hull structures in passenger ships. DNVGL-CG-0138.

Duddeck F. 2008. Multidisciplinary optimization of car bodies. Struct Multidiscip Optim. 35:375-389.

Duysinx, P. and Bendsoe, M.P., "Topology optimization of continuum structures with local stress constraints", International Journal for Numerical Methods in Engineering, Vol. 43, 1998, pp. 1453-1478.

Ehlers S. 2010. A procedure to optimize ship side structures for crashworthiness. J of Eng for the Marit Environ. 224:1-11.

Fransman J. 1988. The influence of passenger ship superstructures on the response of the hull girder. Trans RINA. 131:1-12.

Heder M, Ulfvarsson A. 1991. Hull beam behavior of passenger ships. Marine Struct. 4: 17-34.

Hirakawa S, Kitamura M, Maki M. 2011. Application of genetic algorithm to structural design of 150 KDWT tanker using PrimeShip-HULL rule calculation software. Proceedings of the 21st International Offshore and Polar Engineering conference, Maui, Hawaii (HI), 845-851.

Hughes OF. 1988. Ship structural design: a rationally-based, computer-aided, optimization approach. New Jersey (NJ): Society of Naval Architects and Marine Engineers.

Hughes OF. Mistree F, Zanic V. 1980. A Practical method for the rational design of ship structures. J of Ship Res. 24: 101-113.

ISSC. 1997. Committee II.1 – quasi-static response. Proceedings of the 13th International Ship and Offshore Structures Congress; 1997 Aug 18–22; Trondheim, Norway. pp. 158–165. Oxford (England): Elsevier Science.

Jalkanen J. 2006. Palvelualgoritmi kantavien rakenteiden optimoinnissa [Particle swarm optimization algorithm in load carrying structures design]. Raken Mek. 39(2): 23-35. Finnish.

Kennedy J, Eberhart R. 1995. Particle swarm optimization. IEEE Conf. of neural networks, Piscataway (NJ). 1942-1948.

Klanac A, Ehlers S, Jelovica J. 2009. Optimization of crashworthy marine structures. Marine Struct. 22(4): 670-690.

Marklund PO, Nilsson L. 2001. Optimization of a car body component subjected to side impact. Struct Multidiscip Optim. 21:383-392.

Na SS, Karr DG. 2013. An Efficient stiffness method for the optimum design of ship structures based on common structural rules. Ships and Offshore Struct. 8(1): 29-44

Naar H, Varsta P, Kujala P. 2004. A theory of coupled beams for strength assessment of passenger ships. Marine Struct. 17(8): 590-611.

NX Nastran 7. 2013. Element library reference.

Prebeg P, Zanic V, Vazic B. 2014. Application of a surrogate modeling to the ship structural design. Ocean Eng. 84: 259-272.

Reddy JN. 2004. Mechanics of laminated composite plates and shells – theory and analysis, 2nd ed. Boca Raton (FL): CRC Press.

Richir T, Caprace J-D, Losseau N, Bay M, Parsons MG, Patay S, Rigo P. 2007. Multicriterion scantling optimization of the midship section of a passenger vessel considering IACS requirements. Proceedings of the 10th International Symposium of Practical Design of Ships and Other Floating Structures, Sep 30-Oct 5, Houston (TX), USA, 758-763.

Rigo P. 2009. Least-cost structural optimization oriented preliminary design. J of Ship Prod. 22(4): 202-215.

Ringsberg JW, Saglam H, Sarder Md.A, Ulfvarson A. 2012. Lightweight design of offshore platform marine structures – optimization of weight to strength utilization of corrugated shell plating. Ships and Offshore Struct. 9(1): 38-53.

Romanoff J. 2014. Optimization of web-core steel sandwich decks at concept design stage using envelope surface for stress assessment. Eng Struct 66:1-9.

Romanoff J, Klanac A. 2008. Design optimization of steel sandwich hoistable car decks applying homogenized plate theory. J of Ship Prod. 24(2): 108-115.

Romanoff J, Remes H, Varsta P, Jelovica J, Klanac A, Niemelä A, Bralic S, Naar H. 2013. Hull-superstructure interaction in optimized passenger ships. Ships and Offshore Struct. 8(6): 612-620.

Romanoff J, Varsta P. 2007. Bending response of web-core sandwich plates. Compos Struct. 81: 292-302.

Sekulski Z. 2009. Least-weight topology and size optimization of high speed vehicle-passenger catamaran structure by genetic algorithm. Marine Struct. 22: 671-711.

Sun L, Wang D. 2011. A new rational-based optimal design strategy of ship structure based on multi-level analysis and super-element modeling method. J of Marine Sci Appl. 10: 272-280.

Vasta J. 1958. Lessons learned from full-scale ship structural tests. SNAME Trans. 66: 165-243.

Whitney JM, Pagano NJ. 1970. Shear deformation in heterogeneous anisotropic plates. J of Appl Mech. 37(4): 1031–1036.

Zanic V, Andric J, Prebeg P. 2007. Decision support methodology for concept design of multi-deck ship structures. Proceedings of the 10th International Symposium of Practical Design of Ships and Other Floating Structures, Sep 30-Oct 5, Houston (TX), USA, 468-476.

Zanic V, Andric J, Prebeg P. 2013. Design synthesis of complex ship structures. Ships and Offshore Struct. 8: 383-403.

## Appendix A. Strength criteria

Von Mises yielding criterion is defined for in-plane stress as

$$\sigma_{eq} = \sqrt{\sigma_x^2 + \sigma_y^2 - \sigma_x\sigma_y + 3\tau_{xy}^2},$$

which cannot exceed $245f_1$ when using direct calculation methods, according to DNV (2014). $f_1$ is a material parameter and for steels with the yield strength of 235 MPa and 355 MPa it equals $f_1$=1 and $f_1$=1.39, respectively.

Normal stresses and shear stresses caused by hull girder bending cannot exceed $175f_1$ and $110f_1$, respectively. Buckling of plates is calculated according to DNV using

$$\sigma, \tau = kE\left(\frac{t}{b}\right)^2,$$

where $k$ is the buckling coefficient taking into account the load and boundary conditions and $t$ and $b$ are thickness and breadth of the plate. Corrosion reduction is not used in this work. Johnson-Ostenfeld plasticity correction is applied. Each buckling mode and interaction between different modes is checked. Buckling coefficient $k$ for plates, stiffeners and girders is given in Table 6.

**Table 6. Buckling criteria and coefficients**

| | Longitudinal compression (DNV 2014) | Transverse compression (DNV 2014) | In-plane shear (DNV 2014) | Flexural (DNV 2014) | Torsional (DNV 2014) | Interaction |
|---|---|---|---|---|---|---|
| Plate | 3.62 | 0.9 | 5.34 | | | Bi-axial (DNV 2014) |
| Stiffener | | | | x | x | |
| web | 3.62 | - | 5.34 | - | - | Compression and in-plane bending, compression and shear, shear and in-plane bending (Hughes et al. 1980) |
| flange | 3.62 | - | 5.34 | - | - | Compression and in-plane bending, compression and shear, shear and in-plane bending (Hughes et al. 1980) |